Magnetic phase diagrams and metamagnetic processes in Ising systems: The case of $CeZn_2$

D. Gignoux, P. Morin, and J. Voiron
Laboratoire Louis Néel, CNRS, 166X, 38042, Grenoble CEDEX, France

P. Burlet
Centre d'Etudes Nucléaires de Grenoble, DRF, 85X, 38041, Grenoble CEDEX, France
(Received 25 March 1992)

From magnetization measurements and neutron-diffraction experiments on powders and single crystals, a macroscopic and microscopic description of the complex field-temperature phase diagrams of the Zn-rich $Ce(Zn_{1-x}Cu_x)_2$ orthorhombic compounds is presented. A simple Ising model, involving only three exchange field parameters, gives a quite satisfactory account for the main features of these phase diagrams, namely, (i) the existence of an incommensurate sine wave modulated structure just below T_N, (ii) at low temperature and in zero field the coexistence of two different commensurate antiferromagnetic structures, (iii) the three-step metamagnetic processes along the easy **b** axis at low temperature, (iv) the relative amplitude of the hysteresis associated with the three transitions, hysteresis which does not arise from the anisotropy, but from the exchange interactions.

I. INTRODUCTION

Nowadays particular attention is paid to antiferromagnetic systems, in particular, uniaxial, in which complex magnetic phase diagrams are observed.[1-4] Indeed, multistep metamagnetic processes are observed at low temperature and in zero field several phases are temperature induced below T_N. In particular, one often observes incommensurate modulated structures just below this temperature which transform into equal moment commensurate structures at lower temperatures. Such properties are especially characteristic of a large number of rare-earth-based intermetallic systems on account of the huge uniaxial magnetocrystalline anisotropy and of the long-range and oscillatory character of the exchange interactions [Ruderman-Kittel-Kasuya-Yosida (RKKY) type]. Besides magnetization and susceptibility measurements, neutron diffraction gives a better insight of the microscopic aspects of these phase diagrams, especially on single crystals under applied magnetic field. A careful analysis is then possible which can account for the main features of these complex diagrams. In this context, preliminary studies on $CeZn_2$ and $CeCu_2$ were quite promising. So we have undertaken a study of the magnetic properties and structures of the $Ce(Zn_{1-x}Cu_x)_2$ series. Note that the interest in this study is enhanced by the fact that frequently Ce has an abnormal magnetic behavior such as heavy fermion, intermediate valence, or Kondo effect.

$CeZn_2$ and $CeCu_2$ crystallize in the same orthorhombic $CeCu_2$-type (*Imma* space group) structure.[5] The four Ce atoms of the unit cell belong to the 4*e* site: atoms hence labeled 1, 2, 3, and 4 are in $0,\frac{1}{4},z$, $\frac{1}{2},\frac{3}{4},-\frac{1}{2}+z$, $0,\frac{3}{4},1-z$, and $\frac{1}{2},\frac{1}{4},\frac{3}{2}-z$, respectively. Note that only two Ce atoms belong to the primitive cell (atoms 1 and 3), $CeZn_2$ is antiferromagnetic below $T_N=7.5$ K and the powder neutron-diffraction data have been interpreted with a magnetic cell identical to the crystallographic one and Ce moments of $1.6\mu_B$ along the **b** axis.[6] Later resistivity measurements have shown a Kondo behavior,[7] whereas magnetization on a single crystal exhibits a three-step metamagnetic process when the field is applied along the **b** axis.[7-9] $CeCu_2$ is also a Kondo lattice system which orders antiferromagnetically below 3.5 K.[10] But the low-temperature magnetic properties are quite different from those of $CeZn_2$. Indeed, the easy axis is the **a** direction[11] along which the magnetization process at 1.5 K exhibits a large initial susceptibility with a very smooth metamagnetic transition in low field (≈ 5 kOe).[10,12] Neutron-diffraction experiments on powder were interpreted with a very long-range antiferromagnetic structure[10] in contradiction with the structure deduced from experiments on a single crystal.[13] Indeed, the authors propose a simple antiferromagnetic structure with moments along the **c** axis in contradiction with their magnetization and susceptibility measurements which clearly indicate that **a** is the easy axis. The true structure is probably a very long-range modulation of a simple antiferromagnetic structure with moments along the **a** axis. The study of the magnetic properties of pseudobinary $Ce(Zn_{1-x}Cu_x)_2$ single crystals has shown that the change from the $CeZn_2$-type magnetic behavior to the $CeCu_2$ one occurs in a very small concentration range around $x=0.2$.[8] Crystalline-electric-field (CEF) effects[14] and preliminary results on the field-induced magnetic structures[15] in this series were published recently. In this paper we present the magnetic phase diagram of the Zn-rich compounds of this series studied by means of neutron diffraction on polycrystals and single crystals as well as magnetization measurements on single crystals.

After a brief description of the experimental procedures (Sec. II), we present the low-temperature magnetization measurements and the deduced boundaries between the different regions of the magnetic phase diagrams (Sec. III). Section IV is devoted to the description

of the magnetic structures of the phase diagrams determined from neutron-diffraction experiments. Finally, Sec. V is devoted to an analysis and a discussion of all the results.

II. EXPERIMENT

Single crystals of the compounds with $x=0$, 0.1, 0.15, and 0.25 were grown by the Bridgman technique. On account of the high vapor pressure of Zn, the constituents were first sealed under vacuum in a tantalum crucible and subsequently melted in an induction furnace. From the ingots, cubes of approximately $3\times3\times3$ mm^3 with their faces perpendicular to the **a**, **b**, and **c** axes were spark cut for magnetic and neutron-diffraction measurements. All the neutron-diffraction experiments were performed at the Siloé reactor of the Centre d'Etudes Nucléaires of Grenoble. For the experiments on single crystals, a superconducting cryomagnet which can produce a vertical field up to 80 kOe was mounted on the spectrometer. Magnetization was measured at temperatures from 1.5 to 300 K in fields up to 76 kOe.

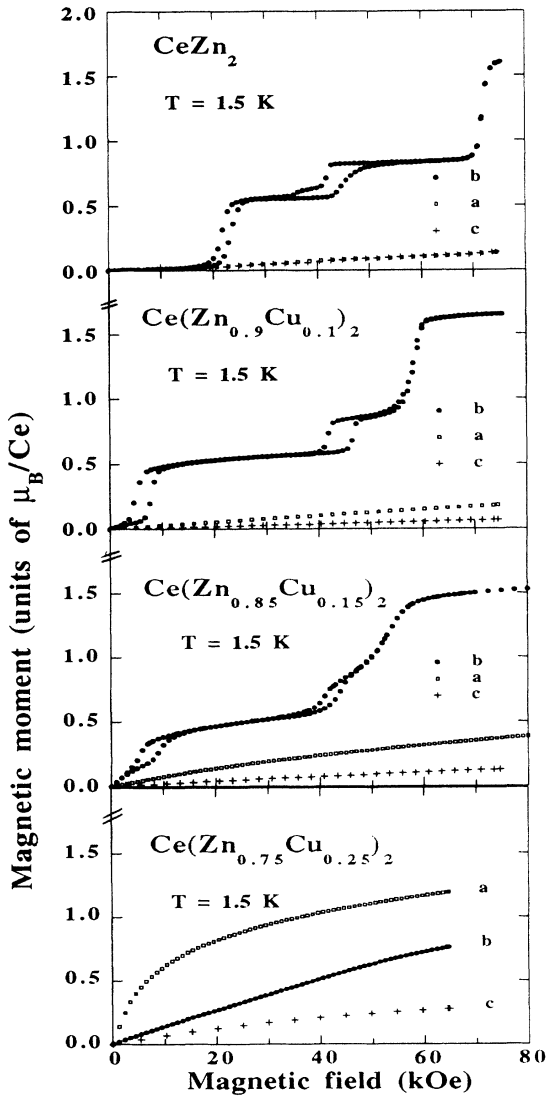

FIG. 1. Magnetization processes at 1.5 K of the $Ce(Zn_{1-x}Cu_x)_2$ compounds with $x=0$, 0.1, 0.15, and 0.25 along the main symmetry axes.

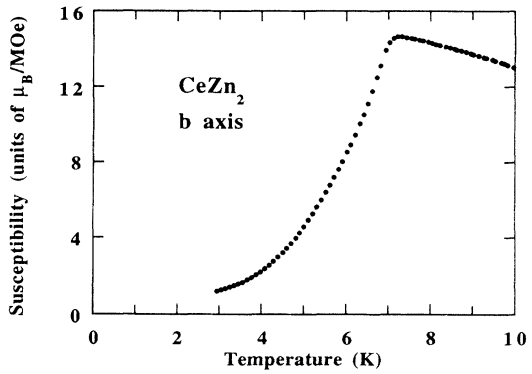

FIG. 2. Thermal dependence of the susceptibility of $CeZn_2$ along the **b** axis.

III. MAGNETIZATION MEASUREMENTS

Figure 1 shows, for single crystals of the four concentrations, the magnetization processes measured at 1.5 K along the three main symmetry axes, i.e., **a**, **b**, and **c**. Two different types of behavior are observed.

Compounds with $x=0.1$, and to a lesser extent, 0.15 are similar to $CeZn_2$. Along **a** and **c** the magnetization is small; it increases slowly and linearly and is always smaller along **c**. Along the **b** axis, which is clearly the easy direction, a three-step metamagnetic process occurs. However, for $x=0$, an additional phase appears in a small field range around 40 kOe: it is only observed in decreasing field at 1.5 K but in increasing and decreasing fields at 4.2 K. Above the highest critical field, the magnetization reaches $1.6\mu_B$, a value which is smaller than that of the free Ce^{3+} ion. This value, which corresponds to the Ce moment previously determined in $CeZn_2$ by powder neutron diffraction,[6] shows that the ferromagnetic state has been reached. In the intermediate phases, magnetizations are near $\frac{1}{3}$ and $\frac{1}{2}$ of the saturation magnetization. For $x=0.15$, the magnetization process is

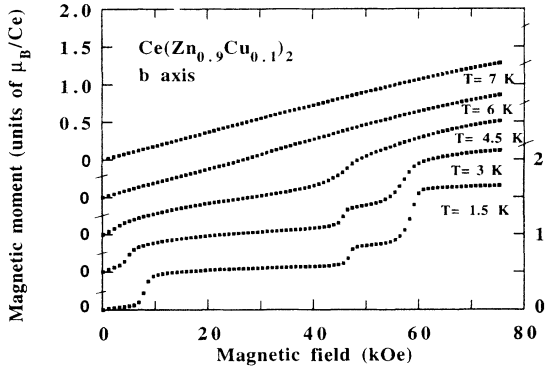

FIG. 3. $Ce(Zn_{0.9}Cu_{0.1})_2$: magnetization process along the **b** axis in increasing field at different temperatures.

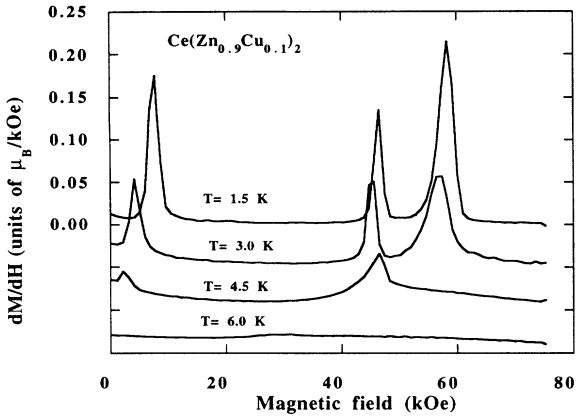

FIG. 4. Field derivative dM/dH along the **b** axis for different temperatures in $Ce(Zn_{0.9}Cu_{0.1})_2$.

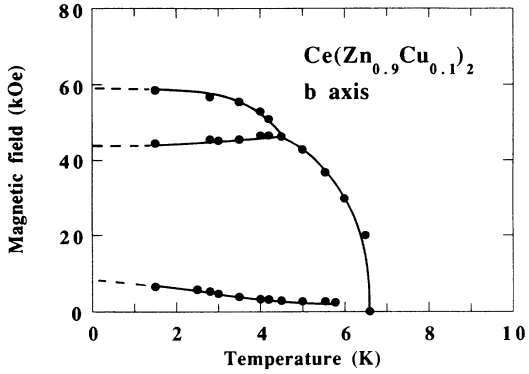

FIG. 6. Magnetic H-T phase diagram of $Ce(Zn_{0.9}Cu_{0.1})_2$ for the **b** direction.

smoothed, making more difficult the determination of the critical fields and of the magnetization in the different phases. It is worth noting that the amplitudes of the hysteresis of the three transitions are quite different: it is very weak for the third one and almost twice as large for the second one than for the first one.

Although the compound with $x=0.25$ does not order down to 1.5 K, the magnetization processes at this temperature are rather similar to those of $CeCu_2$. The easy axis is **a** and the values of the magnetization along the three axes appear to be similar to those of $CeCu_2$. For example, the values of the magnetization measured at 4.2 K in a field of 60 kOe are 1.09 and $1.19\mu_B$ along **a**, 0.60 and $0.72\mu_B$ along **b**, and 0.18 and $0.20\mu_B$ along **c** for $x=0.25$ and $x=1$, respectively. However, the very smooth metamagnetic behavior observed at 1.5 K in $CeCu_2$ has not been observed along any of the axes of $Ce(Zn_{0.75}Cu_{0.25})_2$.

Note that, when x varies from 0 to 0.15, magnetization along **c** is always very small whereas, in a given field, magnetization along **a** increases at least as x^3. Besides, in a 75-kOe applied field, i.e., above the third transition, magnetization along **b** is slightly smaller for $x=0.15$ than for $x=0.10$. This shows that the change of the easy magnetization direction around $x=0.2$ arises from a progressive change of CEF parameters, in particular, B_2^2, as has been deduced from the anisotropy of the paramagnetic susceptibilities.[8,14]

In $CeZn_2$, the low-field susceptibility along **b** exhibits a well-pronounced peak at $T_N=7.5$ K (Fig. 2) and above this temperature the magnetization process does not exhibit any transition. For $x=0.1$, no maximum of the initial susceptibility along this axis is observed at T_N, which has then been determined as the temperature for which no more metamagnetic transitions are observed in the magnetization process. This leads to a Néel temperature of $T_N=6.6$ K, which has been confirmed by neutron diffraction. The evolution of the magnetization processes for $x=0.1$ at different temperatures is shown in Fig. 3. One can see at 7 K a paramagnetic behavior, whereas smooth transitions are still visible at 6 K. As the transitions are smoothed off when the temperature is increased, the thermal dependences of the critical fields have been extracted from the field derivative dM/dH (Fig. 4). The phase diagrams along **b** for $x=0$ and 0.1 are shown in Figs. 5 and 6.

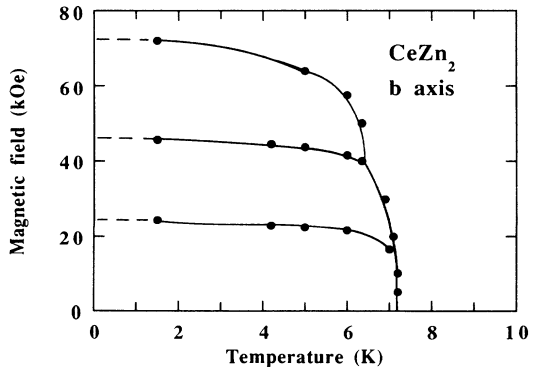

FIG. 5. Magnetic field-temperature H-T phase diagram of $CeZn_2$ for the **b** direction.

IV. NEUTRON DIFFRACTION

A. $Ce(Zn_{0.9}Cu_{0.1})_2$

We have performed neutron-diffraction experiments on this compound (i) for $H=0$ kOe at different temperatures

TABLE I. $Ce(Zn_{0.9}Cu_{0.1})_2$ single crystal at $T=3.9$ K and $H=0$: calculated and observed magnetic intensities. $(hkl^{\pm})$ reflections correspond to the $(h,k,l\pm\tau)$ points of the reciprocal lattice with $\tau=0.61$. The reliability factor and maximum value of the Ce moment are 10.0% and $1.7\pm0.1\mu_B$, respectively.

h	k	l	I_{calc} (10^{-2} b)	I_{obs} (10^{-2} b)
0	0	0^+	15.3	13.8
0	0	2^-	2.0	3.3
0	0	2^+	18.6	20.2
0	0	4^+	7.1	6.1
0	−1	1^+	1.2	1.3
2	0	0^+	11.1	11.0
2	−1	1^+	1.1	1.5

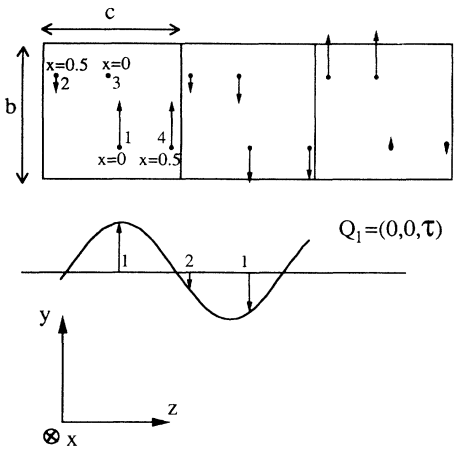

FIG. 7. Modulated magnetic structure of $Ce(Zn_{0.9}Cu_{0.1})_2$ determined at 3.9 K.

ranging from 8 to 1.6 K on a single crystal as well as on a polycrystalline sample, and (ii) on the single crystal at 1.6 K for $H=17.8$ and 47.4 kOe applied along **b**.

In zero field at 8 K, i.e., in the paramagnetic phase, the neutron-diffraction intensities of the nuclear Bragg peaks agree with a random distribution of Zn and Cu atoms on the same $8h$ crystallographic site. A least-squares refinement of the intensities (reliability factor $R=2.3\%$) led to the scaling factor and to the position parameters for Ce ($z=0.552$) and for Zn (or Cu) ($y=0.066$ and $z=0.165$).

Between $T_N=6.6$ and 3.3 K, all the magnetic intensities correspond to an incommensurate propagation vector $\mathbf{Q}_1=(0,0,\tau)$ in a reduced unit with τ near 0.6 and varying continuously with temperature, which proves the incommensurate nature of this ordering. In particular, at 3.9 K, $\tau=0.61$, no third-order harmonics were observed and the refinement of the magnetic intensities (Table I) leads to the sine wave modulated structure shown in Fig. 7.

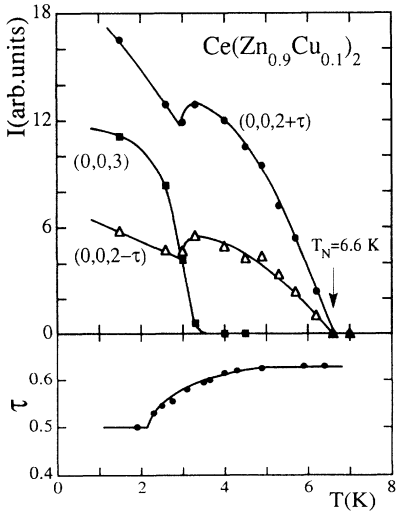

FIG. 8. $Ce(Zn_{0.9}Cu_{0.1})_2$: thermal dependence (i) of neutron-diffraction peaks associated with the propagation vectors $\mathbf{Q}_1$ and $\mathbf{Q}_2$, and (ii) of τ.

TABLE II. $Ce(Zn_{0.9}Cu_{0.1})_2$ single crystal at $T=1.6$ K and $H=0$: calculated and observed magnetic intensities associated with the propagation vector $\mathbf{Q}_2=(0,0,1)$. The reliability factor and Ce moment are 8.2% and $1.6\pm0.1\mu_B$, respectively. This phase was found to occupy 22% of the total volume.

h	k	l	I_{calc} (10^{-2} b)	I_{obs} (10^{-2} b)
0	0	1	7.5	8.1
1	1	1	46.1	48.8
0	1	2	32.7	31.7
1	0	2	22.6	25.7
0	0	3	39.0	34.6
2	0	1	5.4	6.5

Moments 1 and 2, on the one hand (which correspond to each other by a translation of the Bravais lattice), are described by the same sine wave modulation, whereas moments 3 and 4, on the other hand, are described by a modulation with a phase shift of $-70°\pm5°$ with respect to the previous one.

Below 3.3 K, diffraction peaks associated with $\mathbf{Q}_1$ are still present but new peaks which can be indexed with $\mathbf{Q}_2=(0,0,1)$ are also observed [note that, due to the translation $\frac{1}{2},\frac{1}{2},\frac{1}{2}$ associated with the body-centered Bravais lattice, this propagation vector is not equivalent to the (0,0,0) one]. The thermal variation of the intensities of the peaks associated with these two propagation vectors are shown in Fig. 8. The lower part of this figure also shows the thermal dependence of τ which regularly decreases from the maximum value of 0.63 at T_N, reaches the commensurate value $\frac{1}{2}$ at 2 K, and remains locked on this value at lower temperature. The only way to account

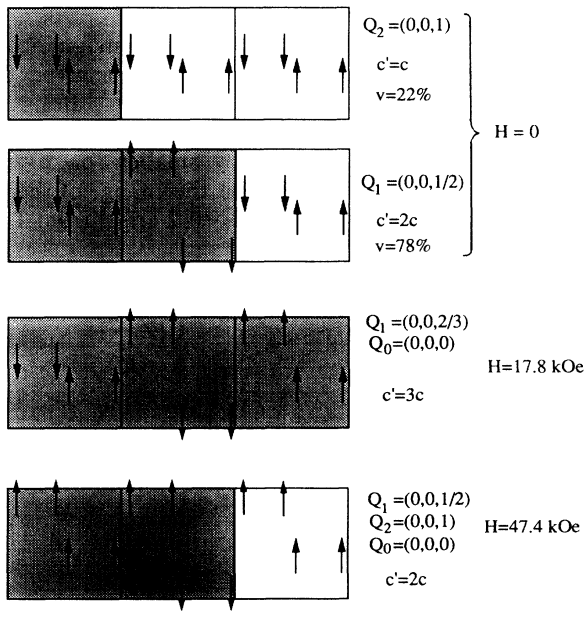

FIG. 9. $Ce(Zn_{0.9}Cu_{0.1})_2$: magnetic structures determined at 1.5 K for $H=0$, 17.8, and 47.4 kOe. The dark areas represent the magnetic cells.

TABLE III. $Ce(Zn_{0.9}Cu_{0.1})_2$ single crystal at $T=1.6$ K and $H=0$: calculated and observed magnetic intensities associated with the propagation vector $\mathbf{Q}_1=(0,0,\frac{1}{2})$. The reliability factor and Ce moment are 12.0% and $1.6\pm0.1\mu_B$, respectively. This phase was found to occupy 78% of the total volume.

h	k	l	I_{calc} (10^{-2} b)	I_{obs} (10^{-2} b)
0	0	$\frac{1}{2}$	24.7	22.3
1	0	$\frac{1}{2}$	11.7	10.2
1	1	$\frac{1}{2}$	8.5	6.4
2	0	$\frac{1}{2}$	17.9	23.5
0	0	$\frac{3}{2}$	3.0	3.2
1	0	$\frac{3}{2}$	29.7	28.1
2	0	$\frac{3}{2}$	2.2	2.9
0	0	$\frac{5}{2}$	30.9	32.1

for the presence, at low temperature, of these two sets of magnetic contributions, in particular, if one assumes that all moments should have the same value, is to consider that the sample is divided into two types of regions, each one being associated with one propagation vector. Within this assumption we have found at 1.6 K the structures shown in Fig. 9. Assuming the same magnetic moment in both phases, the refinement of the intensities (Tables II and III) led to a Ce magnetic moment of $1.6\pm0.1\mu_B$ and to an amount of 78 and 22 % for the $\mathbf{Q}_1$ and $\mathbf{Q}_2$ phases, respectively. Note that the structure associated with $\mathbf{Q}_2$ is the same as that previously reported for $CeZn_2$.[6] A confirmation of this mixing of two different magnetic phases at low temperatures was given from neutron-diffraction experiments on a powder sample in which the amount of both phases was found different: 67 and 33 % for $\mathbf{Q}_1$ and $\mathbf{Q}_2$, respectively.

At 1.6 K for $H=17.8$ kOe along **b** (i.e., in the first field-induced phase) neutron-diffraction peaks, in addition to an increase of the nuclear peaks arising from the induced ferromagnetic component $\mathbf{Q}_0=(0,0,0)$, corresponding to the propagation vector $\mathbf{Q}_3=(0,0,\frac{2}{3})$ were observed. Due to the relative weakness of the ferromagnetic contribution to the nuclear peak, the ferromagnetic component was taken from the magnetization measurements. The refinement of the intensities (Table IV) associated with $\mathbf{Q}_3$ led to the magnetic structure shown in Fig. 9 and to a Ce moment of $1.7\pm0.1\mu_B$. In agreement with magnetization measurements, the first transition thus corresponds to the flipping of $\frac{1}{3}$ of the magnetic moments which were initially antiparallel to the field.

TABLE IV. $Ce(Zn_{0.9}Cu_{0.1})_2$ single crystal at $T=1.6$ K and $H=17.8$ kOe applied along **b**: calculated and observed magnetic intensities associated with $\mathbf{Q}_3=(0,0,\frac{2}{3})$. The reliability factor and Ce magnetic moment are 8.7% and $1.7\pm0.1\mu_B$, respectively.

h	k	l	I_{calc} (10^{-2} b)	I_{obs} (10^{-2} b)
2	−1	$\frac{1}{3}$	21.0	21.1
0	0	$\frac{2}{3}$	17.7	19.9
2	0	$\frac{2}{3}$	12.7	14.5
1	−1	$\frac{2}{3}$	14.2	14.1
1	0	$\frac{5}{3}$	25.4	28.2
0	−1	$\frac{5}{3}$	6.0	5.7
2	−1	$\frac{5}{3}$	5.5	5.1
0	0	$\frac{8}{3}$	30.3	31.5
1	−1	$\frac{8}{3}$	0.8	0.1
0	0	$\frac{10}{3}$	7.9	6.7
0	0	$\frac{14}{3}$	15.8	12.4

TABLE V. $Ce(Zn_{0.9}Cu_{0.1})_2$ single crystal at $T=1.6$ K and $H=47.4$ kOe applied along **b**: calculated and observed magnetic intensities. The reliability factor and Ce moment are 6.1% and $1.7\pm0.1\mu_B$, respectively.

h	k	l	I_{calc} (10^{-2} b)	I_{obs} (10^{-2} b)
0	0	1	2.1	2.0
0	0	3	10.8	10.4
2	0	1	1.5	1.6
1	0	2	6.3	6.4
2	−1	0	13.4	13.6
2	−1	2	7.7	7.8
0	0	$\frac{1}{2}$	13.7	14.4
2	0	$\frac{1}{2}$	9.9	11.1
1	−1	$\frac{1}{2}$	4.7	4.7
2	−1	$\frac{1}{2}$	8.8	8.9
0	0	$\frac{3}{2}$	1.6	1.9
1	0	$\frac{3}{2}$	16.4	17.4
0	−1	$\frac{3}{2}$	1.1	1.2
0	0	$\frac{5}{2}$	17.1	18.3
0	0	$\frac{7}{2}$	1.7	1.2
0	0	$\frac{9}{2}$	6.7	5.2

At 1.6 K for $H=47.4$ kOe along **b**, i.e., in the second field-induced phase, neutron-diffraction peaks appear, in addition to the increase of the nuclear peaks arising from the induced ferromagnetic component $\mathbf{Q}_0$, corresponding to the two propagation vectors $\mathbf{Q}_1=(0,0,\frac{1}{2})$ and $\mathbf{Q}_2=(0,0,1)$. These three propagation vectors are not independent and correspond to harmonics of the same structure. For sake of simplicity we carried out the refinement (Table V) in a magnetic cell twice as large as the crystallographic one along **c**, and we have deduced the magnetic structure shown in Fig. 9. The magnetic moment is $1.7\pm0.1\mu_B$ and the magnetic structure corresponds to the flipping of $\frac{1}{2}$ of the magnetic moments which were initially antiparallel to the field. This value of the magnetic moment is then in agreement with that deduced from magnetization measurements.

B. $CeZn_2$

To study more in depth the thermal dependence of the zero-field magnetic structure of $CeZn_2$, and, in particular to investigate the possibility of an incommensurate phase (as for $x=0.1$) near $T_N=7.5$ K, we have carried out neutron-diffraction patterns on a polycrystalline sample in the temperature range 8–1.8 K. As for the compound

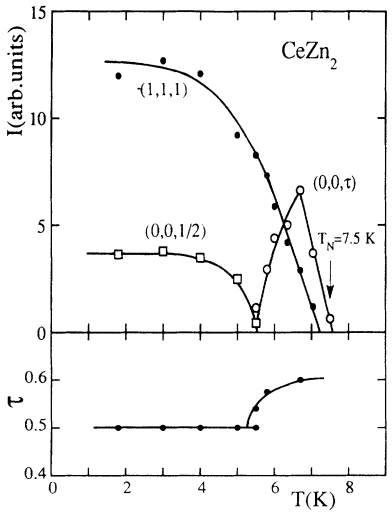

FIG. 10. $CeZn_2$: thermal dependence (i) of neutron-diffraction peaks associated with the propagation vectors $\mathbf{Q}_1$ and $\mathbf{Q}_2$, and (ii) of τ.

with 10% Cu, below T_N, in addition to the contribution associated with $\mathbf{Q}_2$, one observes magnetic peaks which are indexed with the propagation vector $\mathbf{Q}_1$ (this additional contribution was not mentioned in the first neutron-diffraction study[6]). The thermal dependence of the intensity of two peaks associated with each of these vectors is reported in Fig. 10, as well as the thermal dependence of τ (lower part). The main features of these results are the following. (i) The $\mathbf{Q}_2$ phase does not exist between T_N and 7.2 K, and the incommensurate phase is the only one present in this very small temperature range. (ii) τ, which reaches 0.60 at T_N, decreases with temperature and locks on $\frac{1}{2}$ below 5 K. (iii) Except near T_N, the $\mathbf{Q}_2$ phase represents the largest amount and at 1.8 K one finds 9 and 91 % of the $\mathbf{Q}_1$ and $\mathbf{Q}_2$, phases respectively. Because of the similitude of the magnetization processes of both compounds with $x=0$ and 0.1, and owing to the above powder diffraction results, we have concluded that the field-induced magnetic structures were the same. So, we did not determine the additional phase which has been mentioned above to appear in a small range of field around 40 kOe.

V. ANALYSIS AND DISCUSSION

Neutron-diffraction experiments allowed us to determine the microscopic aspects of the magnetic phase diagram of the $Ce(Zn_{1-x}Cu_x)_2$ compounds rich in Zn. The existence of an incommensurate modulated magnetic structure just below T_N, which transforms toward a commensurate equal moment structure at low temperature, is a common feature of rare-earth-based intermetallics.[3] However, in the present study there is a coexistence of two distinct phases below a given temperature: an equal moment one $[\mathbf{Q}_2=(0,0,1)]$ and an incommensurate modulated one $[\mathbf{Q}_1=(0,0,\tau)]$, that, on cooling, progressively transforms toward a commensurate one $(\tau=\frac{1}{2})$ with equal moments. This coexistence means that the energies of the $\mathbf{Q}_1$ and $\mathbf{Q}_2$ phases are very close. The incommensurate propagation vector of the $\mathbf{Q}_1$ phase just below T_N corresponds to the value of $\mathbf{q}$ for which the Fourier transform on the exchange interactions $J(\mathbf{q})$ is maximum. Its change to a commensurate value at low temperatures arises from the effect of higher-order harmonics $J(n\mathbf{q})$ and higher-order terms of the order parameter which play an increasing role when the temperature is decreased if, in agreement with crystal-field effects which lead to a magnetic ground state, moments tend to be equal in order to reduce entropic effects associated with the modulation.

It is worth noting the increase, with the amount of Cu, of the volume of the $\mathbf{Q}_1$ phase at low temperature as well as the temperature range for which the modulated phase is the only one present.

As quoted above, CEF effects in these compounds have been studied by simultaneously analyzing the inelastic-neutron-scattering spectra and the thermal dependences of the paramagnetic susceptibilities along the **a**, **b**, and **c** axes.[14] For $x=0$ and 0.1, the five parameters characterizing these CEF effects on a Ce^{3+} ion in orthorhombic symmetry lead to a magnetic moment of $1.5\mu_B$ in a field of 80 kOe. This value is very close, although slightly smaller, to the observed one $(1.6\mu_B)$. This means that the reduction of the Ce moment compared to the free-ion value $(2.14\mu_B)$ is due to the CEF effects and not to the Kondo effect. These CEF parameters strongly favor the **b** axis which supports the assumption of an Ising-like system used in the analysis presented below.

Due to the great variety of magnetic structures with different propagation vectors, the low symmetry, and the fact that the unit cell contains Ce atoms on two Bravais

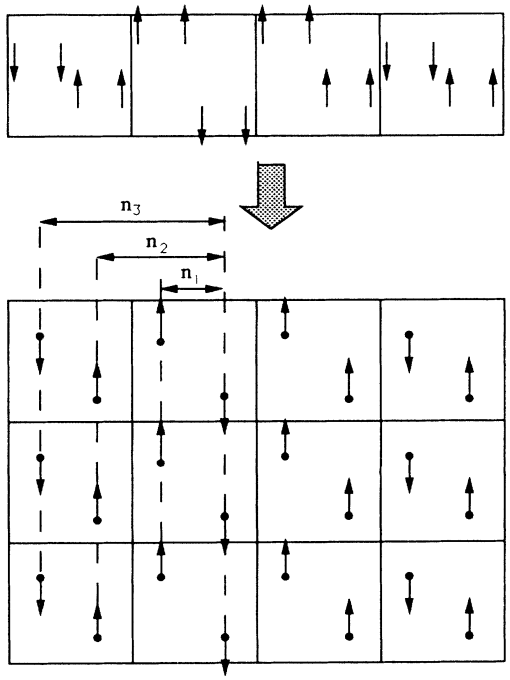

FIG. 11. Sketch showing the equivalent lattice of pairs used in the model of interactions in the case of the first field-induced phase.

lattices, a quantitative interpretation of the magnetic phase diagram of these compounds in terms of exchange interactions can be carried out only by doing some simplifications. The main one uses the following characteristic common to all the observed magnetic arrangements: moments of atoms 1 and 4, on the one hand, and 2 and 3, on the other hand, are always parallel. Even in the modulated structure the phase shift of $-70°\pm5°$ is such that moments 1 and 4 (and 2 and 3) are parallel with close values except, of course, when they are near zero (see the upper part of Fig. 7). This shows that the interaction within each pair of moments is ferromagnetic and larger in magnitude than the other interactions. We have thus considered each of these pairs as a whole and replaced them by a single magnetic moment as shown in Fig. 11 for the first field-induced structure. The subsequent steps of our model are the following: (1) Because of the huge uniaxial CEF anisotropy these compounds are Ising-like systems with a well-defined (for temperatures low enough) moment $\mathbf{M}_0$ being either parallel or antiparallel to **b**. (2) Let n_1M_0, n_2M_0, and n_3M_0 be the molecular fields due to the nearest planes perpendicular to **c** on the plane taken as reference (see Fig. 11). With this tool we can discuss the main features of the magnetic phase diagram.

A. Critical fields

At 0 K, the magnetic energy per Ce atom of the different phases can be written as

$$E_0=n_2M_0^2,\quad E_0'=(n_1-n_2+n_3)M_0^2\ ,$$

$$E_1=\tfrac{1}{3}(n_1+n_2-3n_3)M_0^2-\tfrac{1}{3}M_0H\ ,$$

$$E_2=-\tfrac{1}{2}M_0H\ ,$$

and

$$E_3=-(n_1+n_2+n_3)M_0^2-M_0H\ ,$$

where E_0 and E_0' refer to the zero-field structures with $\mathbf{Q}_1$ and $\mathbf{Q}_2$, respectively. E_1, E_2, and E_3 correspond to the structures induced in increasing field. The coexistence of two structures in zero field means that E_0 and E_0' are almost the same. Assuming that these energies are equal leads to $n_3=2n_2-n_1$. Subsequently, from the comparison of the different energies, we can deduce the different critical fields:

TABLE VI. Low-temperature molecular fields in the $Ce(Zn_{1-x}Cu_x)_2$ compounds with $x=0$ and 0.1.

Compound	$CeZn_2$	$Ce(Zn_{0.9}Cu_{0.1})_2$
n_1M_0 (kOe)	−20.0	−17.7
n_2M_0 (kOe)	−12.0	−9.7
n_3M_0 (kOe)	−4.0	−1.7
H_{c1}^{calc} (kOe)	15.7	6.8
H_{c2}^{calc} (kOe)	40.3	44.6
H_{c3}^{calc} (kOe)	72.0	58.5

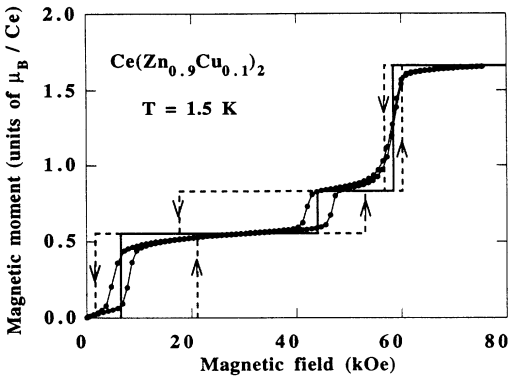

FIG. 12. Calculated and experimental variations of magnetization along **b** at 1.5 K in the compound with $x=0.1$.

$$H_{c1}=4n_1M_0-8n_2M_0\ ,$$

$$H_{c2}=-8n_1M_0+10n_2M_0\ ,$$

and

$$H_{c3}=-6n_2M_0\ .$$

The n_2 parameter can be determined from H_{c3}, whereas n_1 is determined in order to give the best account of the two first critical fields. The values obtained are reported in Table VI. From this table and from Fig. 12 one can see that this model gives quite a satisfactory account of the low-temperature phase diagram. The field dependences of the different calculated energies for the $x=0.1$ compound are shown in Fig. 13; they illustrate well the successive field-induced structures.

B. Hysteresis

At 1.6 K, metamagnetic processes in the compounds with $x\leq0.15$ exhibit hysteresis. The amplitude of this hysteresis is different for each transition; in particular, for the two compounds with $x=0$ and 0.1, this amplitude is very weak for the third transition whereas it is two times larger for the second transition than for the first one. It is then interesting to understand the origin of such characteristics. At 0 K, and in the absence of any activation phenomenon, the transition from one phase to

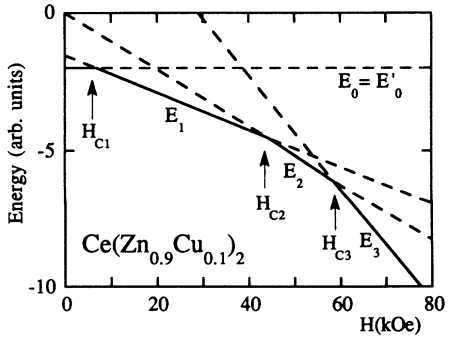

FIG. 13. Calculated field dependence of the magnetic energy for $Ce(Zn_{0.9}Cu_{0.1})_2$.

TABLE VII. Theoretical critical fields and hysteresis of the three transitions.

Transition	H_c^+	H_c^-	ΔH_c
1	$(n_0-2n_2)M_0$	$(-n_0+2n_1-4n_2)M_0$	$2(n_0-n_1+n_2)M_0$
2	$(n_0-4n_1+2n_2)M_0$	$(-n_0-2n_2)M_0$	$2(n_0-2n_1+2n_2)M_0$
3	$(n_0-6n_2)M_0$	$(-n_0-6n_2)M_0$	$2n_0M_0$

the other needs to overcome an energy barrier. Indeed, in order for the structure to change from, say, phase I to phase II, an energy smaller for phase II than for phase I is not enough. This energy barrier does not come from the anisotropy because the latter is too high for the flipping process to take place through a rotation. Indeed, the anisotropy field deduced from the magnetization processes is of the order of 800 and 730 kOe at 1.5 K for $x=0$ and 0.1, respectively. Moreover, such a process would lead to comparable hysteresis for the three transitions. Therefore, the metamagnetic process is driven by the change sign of the total (applied plus molecular) field acting on the flipping moments. One can then calculate the theoretical critical values of H_c^+ and H_c^- for increasing and decreasing fields, respectively. These values are reported in Table VII, where n_0M_0 is the molecular field arising from moments of the same plane. On the same table we have also reported the amplitude of the hysteresis $\Delta H_c=H_c^+-H_c^-$. Replacing n_1M_0 and n_2M_0 by their values (Table VI) gives the different ΔH_c values which are reported in Table VIII where they are compared with the experimental ones for the $x=0.1$ compound. From this table we make the following comments: (i) If one considers that n_0 is small, the calculation accounts for the small value of $\Delta H_{c3}^{\rm obs}$ and for a value of $\Delta H_{c2}^{\rm obs}$ almost twice as large as that of $\Delta H_{c1}^{\rm obs}$. (ii) Knowing that n_0 is certainly positive, the experimental values for transitions 1 and 2 are much smaller than the calculated one. (iii) Assuming $n_0M_0=1.7$ kOe leads to the same ratio between observed and calculated values (about 0.15) for the three transitions. Such a reduction may be driven by identical activation effects. (iv) With this n_0M_0 value, the expected metamagnetic process for $x=0.1$ in increasing and decreasing fields, drawn in Fig. 12, exhibits a large assymmetry in the hysteresis with respect to the critical field H_c corresponding to the simple crossing of energies in the absence of any hysteresis. For instance, $H_{c1}^+-H_{c1}=14.2$ kOe, whereas $H_{c1}-H_{c1}^-=1.6$ kOe. Further experiments of the magnetic aftereffect would allow a more precise study of thermal activation effects in the energy barrier crossing as well as the existence of any other temperature-independent phenomenon. Therefore, in spite of the approximations of the model, one can assert that the origin of the hysteresis loops is the energy associated with exchange interactions.

TABLE VIII. $Ce(Zn_{0.9}Cu_{0.1})_2$: Comparison between the observed and calculated hysteresis for the three transitions. For the calculation, a value of 1.7 kOe for n_0M_0 was used. Values are in kOe.

Transition	$\Delta H_c^{\rm calc}$	$\Delta H_c^{\rm obs}$
1	$16+2n_0M_0=19.4$	3.0
2	$32+2n_0M_0=35.4$	4.9
3	$2n_0M_0=3.4$	0.5

C. $J(q)$ and the high-temperature incommensurate phase

Another interesting aspect of our analysis concerns the thermal evolution of the zero-field magnetic structures. It is well known that the propagation vector of a magnetic structure just below T_N is that for which the Fourier transform $J(\mathbf{q})$ of the exchange interactions is maximum. Such a function for $\mathbf{q}$ parallel to $\mathbf{c}$ (z axis) can be built up from the exchange field coefficient n_i's used above. Let us use the formalism

$$J(\mathbf{q})=\sum_{i\neq j} J_{ij}e^{2\pi i\mathbf{q}(\mathbf{r}_j-\mathbf{r}_i)}$$

when the J_{ij}'s are related to the exchange field by the formula

$$\mathbf{H}_{\rm ex}=\frac{1}{g_J^2\mu_B^2}\sum_{j\neq i} J_{ij}\langle\mathbf{M}(j)\rangle\ .$$

If one neglects the interactions arising from fourth-neighbor equivalent planes, one obtains, in our system,

$$\begin{aligned}J(q_z)&=A[n_0+2n_1\cos(\pi q_z)+2n_2\cos(2\pi q_z)\\&\quad+2n_3\cos(3\pi q_z)]\\&=\frac{A}{M_0}[n_0M_0+2n_1M_0\cos(\pi q_z)\\&\quad+2n_2M_0\cos(2\pi q_z)+2n_3M_0\cos(3\pi q_z)]\ ,\end{aligned}$$

where $A=0.362$ if $J(q_z)$ is expressed in K and consider-

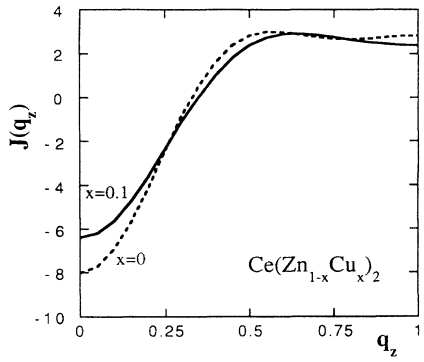

FIG. 14. q_z dependence of $J(\mathbf{q})$ calculated from the deduced exchange field parameters.

ing M_0 as the moment of one pair expressed in μ_B, i.e., twice the Ce moment. This second expression is valid at any temperature provided that the value of M_0 in the denominator and of the $n_i M_0$'s are taken at the same temperature. Using the $n_i M_0$ values of Tables VII and VIII, $M_0 = 3.2\mu_B$, we have plotted in Fig. 14 $J(q_z)$ versus q_z for the compounds with $x=0$ and 0.1. These variations lead us to very interesting conclusions.

(i) $J(q_z)$, which first strongly increases with q_z, does not vary significantly for $0.5 \leq q_z \leq 1$ and has almost the same value for the propagation vectors $\mathbf{Q}_1$ and $\mathbf{Q}_2$.

(ii) $J(q_z)$ is the maximum for $q_z = 0.57$ and 0.63 for $x=0$ and 0.1, respectively. These values are very close to those found experimentally at T_N for both compunds, namely, $q_z = 0.60$ and 0.63, respectively.

D. Further comments

It would be interesting to compare $J(\mathbf{q})$ and $J(0)$ with the Néel temperature and with the paramagnetic Curie temperature without the CEF (although this latter temperature is affected by the Kondo effect). However, such an approach is impossible because of the simplifying assumption which does not take into account the positive interaction (expected to be rather important) between both moments of each pair and which can have an important contribution to these two temperatures.

The present study shows the importance of neutron-diffraction experiments in the determination of magnetic phase diagrams, in particular, to account for the mixing of two different phases in low fields. Due to its macroscopic aspects, the magnetic phase diagram determined from bulk magnetic measurements (bulk phase diagram) cannot give us useful information in this low-field region. For $CeZn_2$, the $\mathbf{Q}_2$ phase occupies more than 90% of the volume and the bulk magnetic properties are characteristic of this phase. In particular, they give an ordering temperature of 7.2 K (Figs. 2 and 5). Actually, this temperature corresponds to the disappearance of the $\mathbf{Q}_2$ phase, whereas between 7.2 and the true value of $T_N = 7.5$ K, determined by neutron diffraction, the compound has the incommensurate $\mathbf{Q}_1$ structure (see Fig. 10). For the compound with $x=0.1$, the amount of each phase is comparable, leading to a bulk magnetic phase diagram still more difficult to interpret without the neutron study. In addition to the lack of a susceptibility anomaly at T_N previously mentioned, this diagram (Fig. 6) does not give any indication of (i) the temperature (2.0 K) above which the $\mathbf{Q}_1$ structure becomes incommensurate and (ii) the temperature (3.3 K) above which the incommensurate phase is not the only one present (see Fig. 8).

As a conclusion, macroscopic and microscopic characteristics of the complex magnetic phase diagrams of the Zn-rich $Ce(Zn_{1-x}Cu_x)_2$ compounds are presented and discussed. An Ising-like model using a set of three exchange field parameters accounts simultaneously for (i) the different magnetic structures observed, their magnetic propagation vectors, and their thermal evolution, as well as the coexistence of two magnetic structures of equivalent energies at low temperature and (ii) the critical fields and the associated hysteresis in the magnetic processes. This system appears to be a good candidate to study the origin of the hysteresis in uniaxial antiferromagnets.

[1]J. Rossat-Mignod, P. Burlet, L. P. Regnault, and C. Vettier, J. Magn. Mater. **90&91**, 5 (1990).
[2]M. Date, J. Magn. Magn. Mater. **90&91**, 1 (1990).
[3]D. Gignoux and D. Schmitt, J. Magn. Magn. Mater. **100**, 99 (1991).
[4]J. A. Blanco, D. Gignoux, D. Schmitt, and C. Vettier, J. Magn. Magn. Mater. **97**, 4 (1991).
[5]E. J. Duwell and N. C. Baeziger, Acta Crystallogr. **8**, 705 (1955).
[6]D. Debray, M. Sougi, and P. Meriel, J. Chem. Phys. **56**, 4325 (1972).
[7]M. Yamashita, M. Kurisu, H. Kadomatsu, I. Oguro, and H. Fujiwara, J. Phys. Soc. Jpn. **56**, 32 (1987).
[8]J. Voiron, P. Morin, D. Gignoux, and R. Aleonard, J. Phys. (Paris) Colloq. **49**, C8-419 (1988).
[9]H. Fujii, M. Akayama, Y. Uwatoka, Y. Hashimoto, and T. Kitai, J. Phys. (Paris) Colloq. **49**, C8-417 (1988).
[10]E. Gratz, E. Bauer, B. Barbara, S. Zemirli, F. Steglich, C. D. Bredl, and W. Lieke, J. Phys. F **15**, 1975 (1985).
[11]S. Takayanagi, Y. Onuki, and T. Komatsubara, J. Phys. Soc. Jpn. **55**, 2384 (1986).
[12]Y. Onuki, Y. Machii, Y. Shimizu, T. Komatsubara, and T. Fujita, J. Phys. Soc. Jpn. **54**, 3562 (1985).
[13]R. Trump, S. Thierfeldt, M. Loewenhaupt, and T. Chattopadhyay, J. Appl. Phys. **69**, 4699 (1991).
[14]P. Morin, D. Gignoux, J. Voiron, and A. P. Murani, Physica B **180-181**, 173 (1992).
[15]D. Gignoux, P. Morin, J. Voiron, and P. Burlet, J. Magn. Magn. Mater. **104-107**, 1262 (1992).

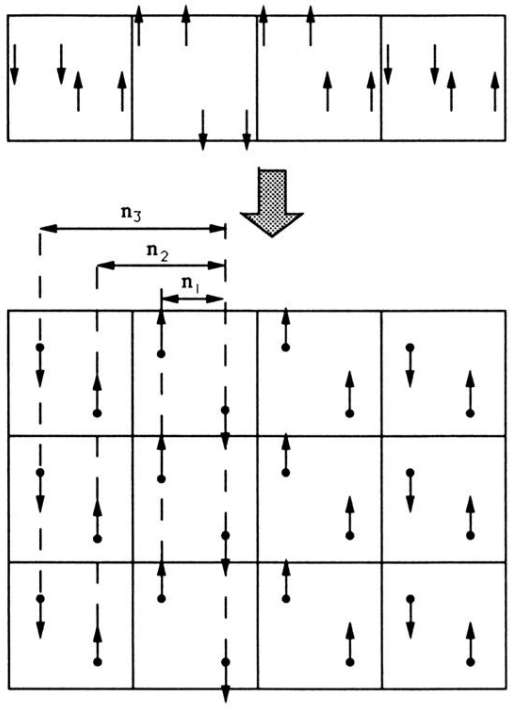

FIG. 11. Sketch showing the equivalent lattice of pairs used in the model of interactions in the case of the first field-induced phase.

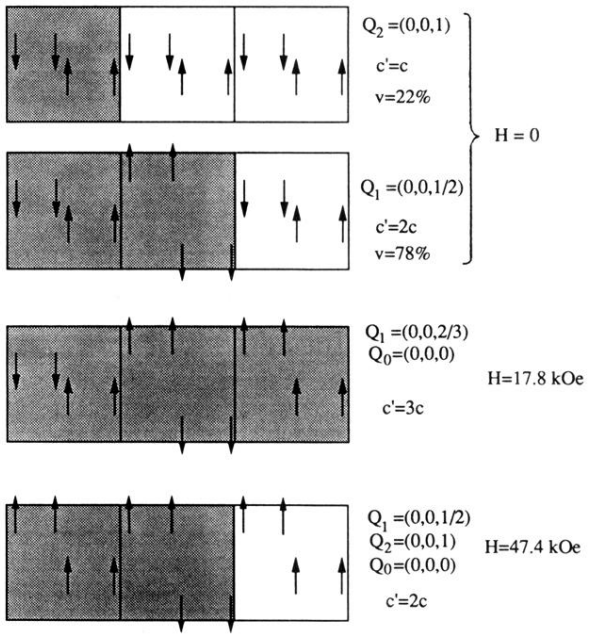

FIG. 9. $Ce(Zn_{0.9}Cu_{0.1})_2$: magnetic structures determined at 1.5 K for $H=0$, 17.8, and 47.4 kOe. The dark areas represent the magnetic cells.